Unique TGFBI Protein in Lattice Corneal Dystrophy

Yu-Ping Han,[1,2] *Austin J. Sim,*[1] *Smita C. Vora,*[1] *and Andrew J. W. Huang*[1]

Purpose. Specific components of transforming growth factor–beta-induced protein (TGFBIp) responsible for amyloid deposits in lattice corneal dystrophy (LCD) have not been delineated. LCD has been associated with various TGFBIp mutations such as R124C, L518P, and L527R. Using recombinant TGFBIp, this study was undertaken to identify TGFBIp components potentially contributing to the protein deposits in LCD.

Methods. Recombinant wild-type (WT) TGFBIp and four mutants (R124C, R124H, L518P, and L527R) were generated in HEK293FT cells. WT and mutant TGFBIp were collected from crude cell lysates or purified from culture media. Immunoblot analyses were performed with four different anti-TGFBIp antibodies raised against various regions of TGFBIp.

Results. Consistent with the authors' previous findings, purified recombinant proteins are more prone to polymerize than crude cell lysates. As expected, all monomers and polymers of TGFBIp WT and mutants were detected by these antibodies. However, the authors noted WT and TGFBIp mutants showed differential reactivities with these antibodies. A 47-kDa band was detected in purified 2-tag proteins of L518P by all four antibodies. A unique 43-kDa band was detected in both 1-tag cell lysates and purified proteins of R124C by the authors' custom-made antibody (KE50) and a commercial anti-TGFBIp.

Conclusions. Based on its universal reactivity with various antibodies, the authors surmise that the 47-kDa protein is a ubiquitous TGFBIp fragment derived from the N-terminus of the L518P mutant. The fact that the 43-kDa protein fragment was present primarily in R124C and R124H but not in WT implicates its potential role in the protein deposits of LCD. (*Invest Ophthalmol Vis Sci.* 2011;52:8401–8406) DOI:10.1167/iovs.11-7618

The transforming growth factor–beta-induced (*TGFBI*) gene, also known as *βigh3* encoding for TGFBIp (also called βigh3 protein, keratoepithelin, or RGD-CAP) was first identified by Skonier et al.[1] from a human lung adenocarcinoma cell line (A 549) that had been treated with TGF-β. TGFBIp is a secretory protein composed of 683 amino acids containing a secretory signal peptide sequence at the N-terminus, four "Fas 1–like " domains (~140 amino acids for each domain) homologous to Drosophila fasciclin-1 (Fas-1), and an arginine–glycine–aspartate (RGD) motif located at the C-terminus. TGFBIp is expressed in a wide range of tissues including the cornea,[2,3] skin,[4] bone,[5] tendon,[6,7] endometrium,[8] and kidney,[9] and it has been reported to interact with various extracellular matrix proteins[10] and promote cell attachment, migration, proliferation, and differentiation, likely via the interaction with integrins. Although the exact biological function of TGFBIp in the cornea remains unclear, numerous mutations of *TGFBI* have been identified to date and linked to at least 13 different phenotypes of corneal epithelial and stromal dystrophies.[11] These autosomal-dominant corneal diseases are characterized by a progressive abnormal accumulation of protein aggregates in the corneal epithelium and stroma, which eventually leads to severe visual impairment.[12]

Although TGFBIp has been shown to colocalize with protein deposits in *TGFBI*-linked corneal dystrophies,[13] the composition of the protein aggregates remains to be characterized in detail. Lattice corneal dystrophy (LCD) is the most common corneal stromal dystrophy characterized with corneal deposits in refractile lattice lines without associated systemic findings. By histology, these corneal deposits are fusiform in shape and amyloid in nature. Almost all types of LCD, except LCD2, have been demonstrated to be attributed to various mutations in the *TGFBI*.[14] According to their clinical characteristics, TGFBIp-related LCDs have been classified into two groups: the early-onset LCDs or LCD1 associated with the Arg124Cys (R124C)[15] and Leu518Pro (L518P)[16] mutations and the late-onset LCDs or LCD3A associated with the Pro501Thr,[17] Leu527Arg (L527R),[18] and Ala546Thr[19] mutations. Furthermore, it has been shown that corneas with LCD have an abnormal degradation pattern of TGFBIp compared with that of normal corneas.[20] Zerovnik et al.[21] proposed that protein conformational change and unfolding to be the prevailing mechanisms for amyloid fibril formation. Stix et al.[22] further confirmed the presence of proteolytic fragments of TGFBIp in the amyloid deposits of LCD1. They suggested that an unstable globular state of the mutated TGFBIp could lead to protein unfolding for proteolytic cleavage and eventually amyloid formation. Proteolysis has also been presented as a mechanism for clearing the pathologic corneal protein aggregates.[22]

Consequent to the recently recognized involvement of protein fibrils in several, mainly neurodegenerative, diseases such as Alzheimer's disease, Huntington's disease, and Parkinson's disease,[23] there have been increasing interests in the field of protein aggregation and fibril formation. Studying the molecular properties of disease-related proteins under amyloid-conducive conditions should shed light on the protein aggregation behavior and related pathogenic pathways. Elucidation of such mechanisms may also help achieve a more comprehensive understanding of the pathogenesis of TGFBIp-related corneal dystrophies. Different staining patterns of normal corneas and TGFBIp-containing deposits have been published, with various antibodies reacting with various portions of the TGFBIp.[2,21,24,25] However, because transgenic animal models have failed to manifest relevant corneal dystrophic phenotypes,[26]

From the [1]Department of Ophthalmology and Visual Sciences, Washington University School of Medicine, St. Louis, Missouri; and the [2]Shanxi Eye Hospital, Taiyuan, Shanxi, China.

Supported in part by National Institutes of Health (NIH) Grant R01EY017609; a Research to Prevent Blindness (RPB) Physician Scientist Award; an unrestricted grant from Horncrest Foundation, Inc. (AJWH); an unrestricted grant from RPB, Inc. awarded to the Department of Ophthalmology and Visual Sciences at Washington University; and NIH Vision Core Grant P30 EY02687.

Submitted for publication March 24, 2011; revised August 12, 2011; accepted September 20, 2011.

Disclosure: **Y.-P. Han**, None; **A.J. Sim**, None; **S.C. Vora**, None; **A.J.W. Huang**, None

Corresponding author: Andrew J. W. Huang, Department of Ophthalmology and Visual Sciences, Washington University School of Medicine, 660 S. Euclid Avenue, Campus Box 8096, St. Louis, MO 63110; huanga@vision.wustl.edu.

studies with recombinant proteins are the appropriate avenue for understanding the amyloid fibril formation by TGFBIp. Using purified recombinant TGFBIp, we have successfully demonstrated the formation of amyloid fibrils in vitro.[27] Additionally, we have recently identified TGFBIp fragments potentially responsible for granular deposits in the TGFBIp-related granular corneal dystrophies (GCD 1 and 2; Han YP, et al., submitted for publication, 2011). The goal of the present study was to further identify unique protein components potentially responsible for amyloid deposits in TGFBIp-related LCD. Using four different anti-TGFBIp antibodies raised against various regions of TGFBIp, we investigated the molecular properties of recombinant WT TGFBIp and three LCD-related mutants (R124C, L518P, and L527R). The R124H mutation of TGFBIp, responsible for GCD 2 but with lattice deposits, was also used for comparison.

Materials and Methods

Production of Recombinant Wild Type and Mutant TGFBI Proteins

To study the role of TGFBIp in corneal dystrophies, we generated recombinant wild type and several mutant TGFBI proteins (R124C, R124H, L527R, and L518P) for comparison.[28] To facilitate purification of recombinant 1-tag TGFBIp (amino acids [a.a.] 30–683), a hexahistidine tag was inserted right after the encoded signal peptide at the 5′-end as previously described.[27] The coding sequence of nearly full-length TGFBIp (a.a. 1–641, resembling the secreted protein with RGD motif removed from the 3′-end) was PCR-amplified from an I.M.A.G.E. clone (Clone I.D. 2957915; GenBank BE206112) and inserted into pIRES.puro3 for stable expression in a mammalian cell line (HEK293FT; Invitrogen, Carlsbad, CA). For 2-tag TGFBIp (a.a. 30–641), a hexahistidine tag and a Strep II tag were inserted right after the encoded signal peptide at the 5′-end and before the RGD motifs of TGFBIp at the 3′-end, respectively. A transfecting reagent (FuGENE 6; Roche) was used to transfect HEK293FT cells, which were maintained in Dulbecco's modified Eagle's medium (DMEM) plus 10% fetal bovine serum (FBS) under puromycin selection (3 μg/mL) post transfection. Individual clones were selected by monitoring their growth rates and TGFBIp expression level (as determined by dot-blot experiments). Clones stably expressing TGFBIp were then cultured in DMEM with reduced puromycin (10% FBS, 1 μg/mL puromycin). For purification of TGFBIp, culture media were sequentially replaced with serum-free media (FreeStyle 293; Invitrogen) over the course of three passages. Secreted TGFBIp (a.a. 30 to 683 or a.a. 30–641) in the conditioned medium was isolated by metal affinity chromatography using a tetradentate chelating resin (HisPur Cobalt Resin; Thermo Scientific). The purified TGFBIp was dialyzed against phosphate buffer and then concentrated by filtration using 50-kDa centrifuge filters. The recombinant TGFBIp was then lyophilized and stored at −80°C. During reconstitution, lyophilized TGFBIp was dissolved in 10 M urea (10 mM phosphate buffer, pH 7.4) for 1 hour at room temperature before being gel-filtered into fresh phosphate buffer to prevent uneven protein aggregation. It was then allowed to aggregate in phosphate-buffered saline (PBS) at 37°C.

To obtain the cell lysates, transfected HEK293FT cells were grown in 100-mm Petri dishes with media as described earlier. When the cells grew to 75–80% confluency, culture medium was removed from the Petri dishes and each plate was rinsed thoroughly with cold PBS buffer. A radioimmunoprecipitation assay buffer (1× PBS; 1% Igepal; 0.1%SDS; 0.5% deoxycholic acid disodium salt) containing fresh protease inhibitor was added to each plate (0.6 mL per 100-mm plate) to lyse the cells. The lysed cells were scraped off the plate with a cell scraper and lysates were collected using a syringe with a 21-gauge needle and transferred to microcentrifuge tubes. Cell lysates were incubated with 10 μL of 10 mg/mL phenylmethylsulfonyl fluoride for 30 to 60 minutes at 4°C. Crude cell lysates were centrifuged at 15,000*g* for 20 minutes at 4°C to remove nuclear fragments and tissue debris. The remaining supernatants were stored at −20°C until used for protein analyses. The supernatants were not dialyzed against phosphate buffer and not further concentrated by filtration. Total protein contents in the cell lysates were measured by Bradford protein assay on aliquots of each supernatant collected.

Gel Electrophoresis and Immunoblotting

Lysate proteins (20 μg/lane) and purified recombinant TGFBI proteins (50 ng/lane) from transfected cells were separated by electrophoresis on 7.5% SDS-PAGE gels (Bio-Rad, Hercules, CA). A commercial full-length recombinant TGFBIp, BIGH3 (a.a. 1–683; R&D Systems, Minneapolis, MN, 50 ng/lane) was used as a positive control. The protein solution was mixed with a concentrated 6 × sample buffer to achieve a final concentration of 31.25 mM Tris-HCl, 1% SDS, 5% glycerol, 5% β-mercaptoethanol, and 0.000625% acid–base indicator/dye (Bromophenol Blue; Sigma-Aldrich). The samples were heated in a water bath at 100°C for 10 minutes before being loaded for electrophoresis. We did not observe any unusual protein aggregates in the sample buffers before electrophoresis. Gel electrophoresis was conducted in a commercial running buffer (from Bio-Rad) with a final concentration of 25 mM Tris, 291 mM glycerin, 0.1% SDS (pH 8.3) with a power supply (Bio-Rad) at 90 volts for 20 minutes and 120 volts for 40 minutes. The separated proteins were transferred to 0.2 μm polyvinylidene fluoride (PVDF) membranes (Bio-Rad) in transfer buffer (10% 10× TGS from Bio-Rad; 70% MilliQ H_2O; 20% methanol) using 0.35A power for 1 hour 15 minutes by making a sandwich with a plastic cassette. After transfer, PVDF membranes were blocked with 0.2% nonfat dry milk in Tris-buffered saline-Tween (TBST) solution (containing 20 mM Tris, pH 7.5; 500 mM NaCl; 0.1% Tween-20) for 1 hour at room temperature and then incubated for 1 hour at room temperature or overnight at 4°C with various anti-TGFBIp antibodies, including a custom-made rabbit polyclonal anti-TGFBIp antibody, KE50, against a.a. 125 to 683 (University of Minnesota, MN) at 1:5000 dilution; a mouse polyclonal anti-TGFBIp antibody, B01, raised against a.a. 1–683 (Abnova Corp., Taipei, Taiwan) at 1:500 dilution; a rabbit polyclonal anti-TGFBIp antibody against a.a. 199–406 (Proteintech Group Inc., Chicago, IL) at 1:500 dilution; and a custom-made rabbit polyclonal anti-TGFBIp antibody, KE2645, raised against a.a. 27 to 45 (University of Minnesota) at 1:5000 dilutions. After blocking, blots were washed three to four times every 15 minutes with TBST and then incubated for 1 hour at room temperature, with corresponding secondary antibodies such as goat anti-mouse or anti-rabbit IgG-HRP (Santa Cruz Biotechnology, Santa Cruz, CA) at 1:20,000 dilution, while the Western C molecular weight (MW) marker was incubated as well (Precision Strep-Tactin-HRP conjugate; Bio-Rad) at 1:30,000 dilution. Blots were washed again and the protein bands were visualized by using an enhanced chemiluminescence (Immobilon Western, Millipore Corp., Billerica, MA) reagent on a film. All immunoblots were repeated at least three times each to confirm our findings and representative blots were included in this report.

Results

As noted in our previous study,[29] our custom-made KE50 could detect the nearly full-length recombinant WT TGFBIp. Herein, we further confirmed that this antibody could detect a distinct 68-kDa band (TGFBIp monomer) and a weaker 140-kDa band (TGFBIp dimer) in the control BIGH3, along with two corresponding bands at 62 kDa (TGFBIp monomer) and 125 kDa (TGFBIp dimer) in all our purified recombinant $(His)_6$-TGFBI-Strep proteins of WT, R124C, R124H, L518P, and L527R (Fig. 1A). Additionally, several higher MW bands (representing oligomeric TGFBIp) were noted in R124C and R124H mutants. It is noteworthy that KE50 also reacted with a cluster of bands in the 40- to 50-kDa range, and two higher MW bands between 62 and 125 kDa in our purified 2-tag L518P mutant

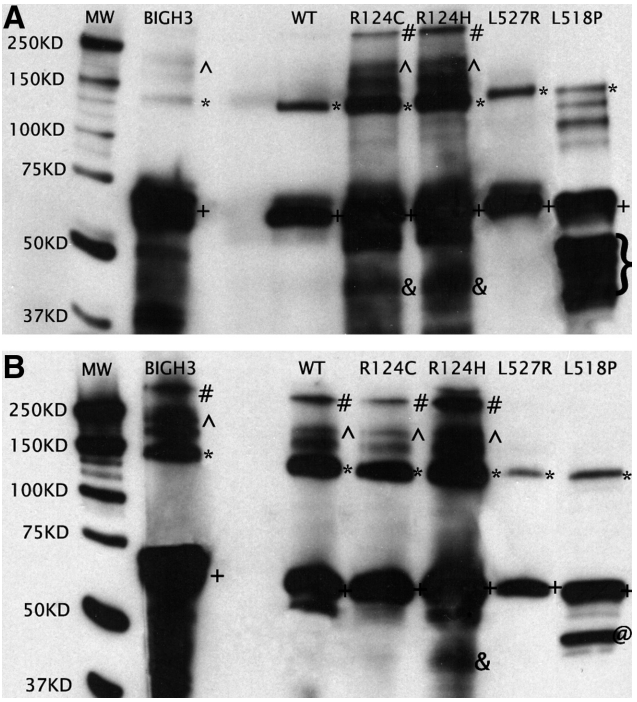

FIGURE 1. Immunoblots of 2-tag recombinant proteins stained with our custom-made polyclonal anti-TGFBIp antibody, KE50 (**A**), and a polyclonal anti-TGFBIp antibody (Abnova Co.; B01) (**B**). (**A**) Immunoblotting of KE50 with purified $(His)_6$-TGFBI-Strep proteins (a.a. 30–641) detected a monomeric 62-kDa band and a less prominent dimeric 125-kDa band in WT, R124C, R124H, L527R, and L518P. This antibody also detected several bands of oligomers with higher molecular weights representing trimers and tetramers in R124C and R124H. Of note, this antibody recognized a cluster of protein bands around 40 to 50 kDa in $(His)_6$-TGFBI-Strep L518P, but not in WT or L527R. There was also a slightly less prominent band around 43 kDa in R124C and R124H. KE50 reacted with a control BIGH3 protein (a.a. 1–683, MW 68 kDa) in a similar pattern with a 68-kDa monomeric band and a faint 140-kDa dimeric band. (**B**) Immunoblotting of B01 with purified $(His)_6$-TGFBI-Strep proteins (a.a. 30–641) detected a monomeric 62-kDa band and a dimeric 125-kDa band in WT, R124C, R124H, L527R, and L518P, similar to those of KE50. This antibody also detected several bands of oligomers with higher molecular weights representing trimers and tetramers in WT, R124C, and R124H. This antibody also detected a 68-kDa monomeric band, a 140-kDa dimeric band, and several oligomeric bands in the control BIGH3 protein in a similar pattern. It is noteworthy that this antibody detected a clear 47-kDa band in L518P, which corresponds to the cluster of 40 to 50 kDa detected by KE50. This antibody also detected a less prominent band around 43 kDa in R124H.

proteins (Fig. 1A). A cluster of fragments with MW of approximately 43 kDa was also noted in R124C and R124H mutants.

To further study the unusual cluster noted in 2-tag L518P, we analyzed the blots with several other anti-TGFBIp antibodies. As expected, a commercial polyclonal anti-TGFBIp antibody (Abnova Co.), B01 (raised against a.a. 1–683, with a similar epitope to our KE50), reacted predominantly with the monomers and dimers of BIGH3 (68 and 140 kDa, respectively) and their corresponding bands (62 and 125 kDa, respectively) in purified 2-tag WT, R124C, R124H, L518P, and L527R (Fig. 1B). Furthermore, this antibody also detected several higher MW bands (representing TGFBIp oligomers) in BIGH3, WT, R124C, and R124H, but not in L527R or L518P protein samples. A slightly less prominent band of approximately 43 kDa was also noted in R124H. Importantly, a clear 47-kDa band was identified by this antibody in purified L518P protein samples. However, B01 did not react with the oligomers of L518P and L527R (Fig. 1B).

To confirm whether this 47-kDa protein fragment is related to bona fide TGFBIp, further investigations were undertaken with two other polyclonal antibodies raised against different regions of TGFBIp. Similar to the two aforementioned antibodies, an anti-TGFBIp antibody (Proteintech Group) (raised against a.a. 199–406) and our custom-made KE2645 (raised against a.a. 27–45) both detected a prominent 62-kDa band in WT and all TGFBIp mutants (Figs. 2A, 2B). These two antibodies also reacted with each TGFBIp dimer to a different extent. Furthermore, a band of approximately 43 kDa in R124H was identified by anti-TGFBIp (Proteintech Group) and a band of approximately 43 kDa was detected by KE2645 in R124C and R124H. It is noteworthy that these two antibodies also detected a clear 47-kDa band in purified L518P protein (Figs. 2A, 2B).

We further speculated if these protein fragments (47 and 43 kDa) were induced by proteolysis. As noted from our previous report,[27] 1-tag proteins are more prone to degrade than the 2-tag proteins. We therefore analyzed the blots from both cell lysates and purified proteins of $(His)_6$-TGFBIp (a.a. 30–683, one tag) for further comparison. We noticed that KE50 reacted predominantly with the monomeric TGFBIp (65 kDa) and to a

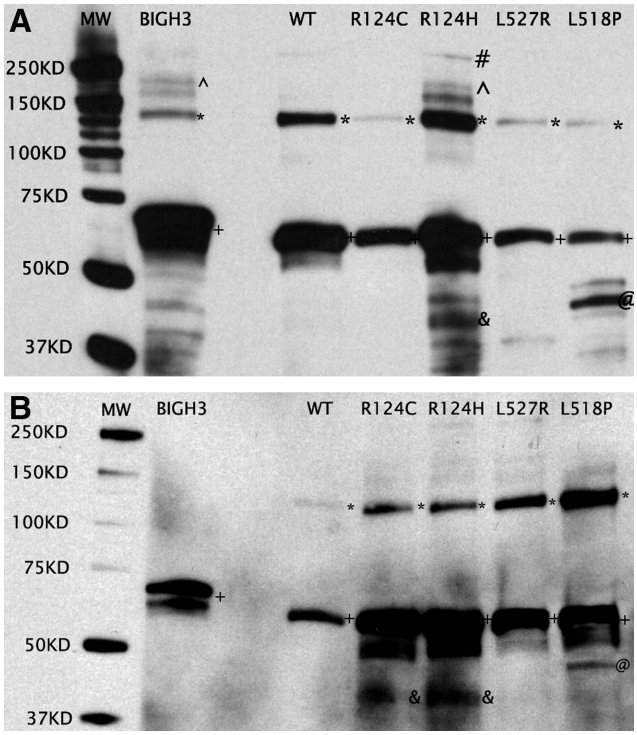

FIGURE 2. Immunoblots of 2-tag recombinant proteins stained with a polyclonal anti-TGFBIp antibody (Proteintech Group [PTG] Co.) (**A**) and another custom-made polyclonal anti-TGFBI antibody, KE2645 (**B**). (**A**) Immunoblotting of PTG antibody with purified $(His)_6$-TGFBI-Strep proteins (a.a. 30–641) revealed a monomeric 62-kDa band and a less prominent dimeric 125-kDa band in WT, R124C, R124H, L527R, and L518P. This antibody also reacted slightly with several bands of oligomers with higher molecular weights representing trimers or tetramers in R124H. Of note, this antibody recognized a clear 47-kDa band in L518P, but not in WT, R124C, or L527R. In addition, there was a less prominent band of 43 kDa in R124H. This antibody also reacted with the monomers and dimers of the commercial BIGH3 protein (a.a. 1–683, MW 68 kDa). (**B**) Immunoblotting of KE2645 with purified 2-tag protein detected a monomeric 62-kDa band and a dimeric 125-kDa band in WT, R124C, R124H, L527R, and L518P, with the dimeric band being relatively faint in WT. It also detects a 47-kDa band in L518P and a band at 43 kDa in R124C and R124H.

lesser extent with the corresponding dimers (130 kDa) in both purified proteins and cell lysates of WT, R124C, R124H, L527R, and L518P (Figs. 3A, 3B). Importantly, KE50 detected a 43-kDa band in the purified 1-tag protein as well as the crude lysates of R124C (Figs. 3A, 3B). In contrast, KE50 did not detect any 47-kDa band in 1-tag protein or cell lysates. It was also evident that the purified recombinant proteins were more prone to aggregate than the cell lysates (Figs. 3A, 3B).

The rabbit polyclonal anti-TGFBIp (Proteintech Group) predominantly reacted with the monomeric 1-tag TGFBIp (65 kDa) and to a much lesser extent with the corresponding dimers (130 kDa) in both purified proteins and cell lysates of WT, R124C, R124H, L527R, and L518P (Figs. 4A, 4B). Moreover, this antibody detected a 43-kDa band in both purified proteins and cell lysates of 1-tag R124C (Figs. 4A, 4B). Neither this antibody nor KE50 detected a 47-kDa band in purified proteins or cell lysates of 1-tag L518P (Figs. 3A, 3B vs. Figs. 4A, 4B).

For comparison, KE2645 detected only a monomeric 65-kDa band in all $(His)_6$-TGFBI (1-tag) purified proteins and cell lysates (a.a. 30–683) (data not shown). On the other hand, B01 (Abnova Co.) detected both monomers and dimers in purified $(His)_6$-TGFBI WT, R124C, R124H, and L527R proteins as well as in cell lysates of R124C and R124H (data not shown). Neither antibody detected the 43-kDa band in the purified proteins or cell lysates of R124C or R124H (data not shown), and neither reacted with the 47-kDa fragment in 1-tag L518P.

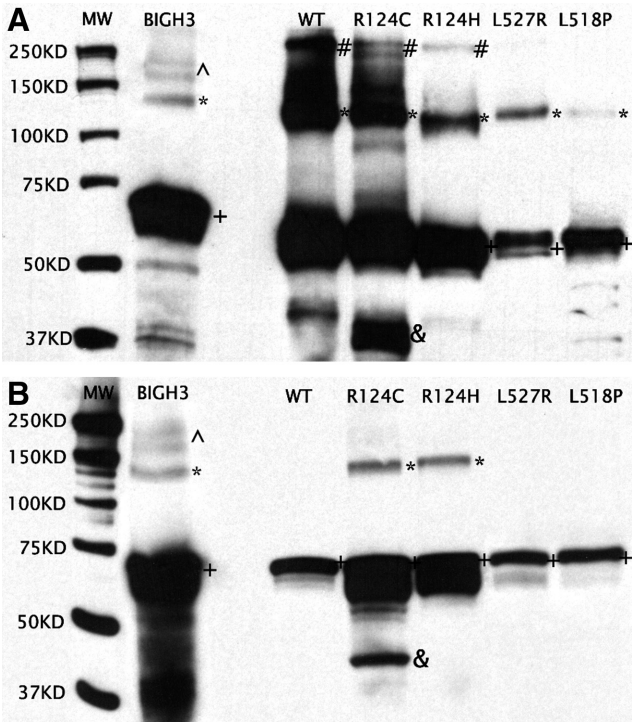

Figure 3. Immunoblots of KE50 with 1-tag proteins (**A**) and cell lysates (**B**). (**A**) Immunoblotting of KE50 with purified $(His)_6$-TGFBI proteins (a.a. 30–683) detected a monomeric 65-kDa band and a dimeric 130-kDa band in WT, R124C, R124H, L527R, and L518P. This antibody also detected several bands of higher molecular weights representing trimers and tetramers in WT, R124C, and R124H. KE50 also recognized a 43-kDa band in 1-tag R124C, but not in WT, L527R, or L518P. There was a very faint 43-kDa band in R124H. (**B**) Immunoblotting of KE50 with 1-tag cell lysates detected a monomeric 65-kDa band in WT, R124C, R124H, L527R, and L518P, and a dimeric 130-kDa band in R124C and R124H. It also detected a 43-kDa band in R124C.

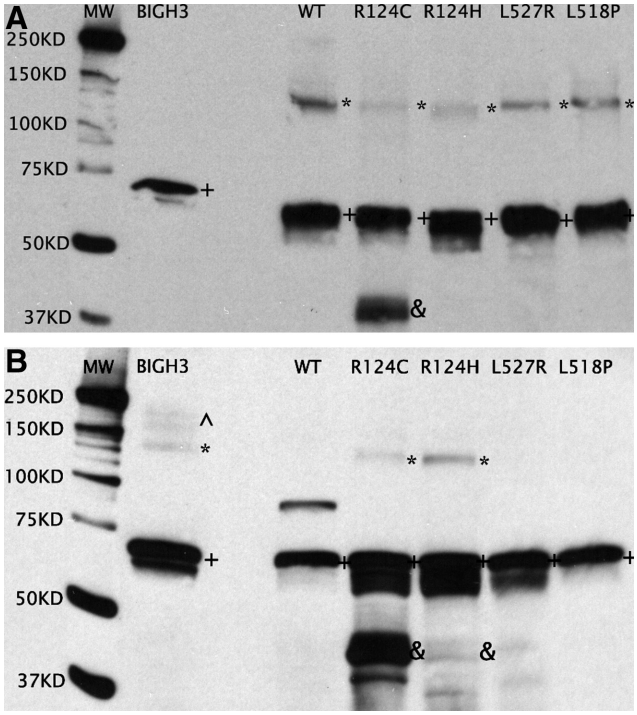

Figure 4. Immunoblots of 1-tag proteins (**A**) and cell lysates (**B**) stained with a polyclonal anti-TGFBIp antibody (PTG). (**A**) Immunoblotting of the PTG antibody with purified $(His)_6$-TGFBI proteins (a.a. 30–683) detected a monomeric 65-kDa band and a less prominent dimeric 130-kDa band in WT, R124C, R124H, L527R, and L518P. Of note, this antibody also detected a clear 43-kDa band in 1-tag R124C. (**B**) Immunoblotting of the PTG antibody with 1-tag cell lysates detected a monomeric 65-kDa band in WT, R124C, R124H, L527R, and L518P, and also recognized a dimeric 130-kDa band in R124C and R124H. Additionally, this antibody detected a prominent 43-kDa band in R124C. A faint 43-kDa band was barely visible in R124H.

Discussion

LCD has been reported to be associated with mutations in the *TGFBI* gene. LCD type 1, in which the most common mutation is R124C, is inherited in an autosomal-dominant fashion, resulting in progressive corneal opacities that lead to severe loss of vision in the fourth or fifth decade. Other uncommon mutations found in families with LCD type 1 include Leu518Pro and Leu509Arg.[30] Evidence indicates that these corneal opacities are caused by amyloid aggregates resulting from the accumulation of TGFBIp and related mutant proteins. The severity of corneal dystrophies correlates well with the extents of mutant TGFBIp aggregations. Korvatska et al.[31] first pointed out that the amyloid and nonamyloid forms of 5q31-linked corneal dystrophy resulting from *TGFBI* mutations at R124 are associated with abnormal turnover of the protein and degradation of mutant TGFBIp. Many proteomic studies have also suggested that the disease-causing proteins form abnormal degradations under physiologic conditions.[32–34]

In our present study, we undertook an in vitro investigation of the potential components of TGFBIp responsible for causing the untoward corneal deposits using a battery of anti-TGFBIp antibodies and several recombinant mutant proteins (R124C, L518P, and L527R) representing the most common genotypes for lattice corneal dystrophies. Recombinant R124H associated with granular corneal dystrophy type 2 (GCD2; also known as Avellino Corneal Dystrophy) and lattice deposits was used for comparison. We further confirmed that our double-tagged recombinant $(His)_6$-TGFBIp-Strep (a.a. 30–641) has a slightly

lower MW of 62 kDa, whereas our single-tagged recombinant $(His)_6$-TGFBIp (a.a. 30–683) has a MW of 65 kDa. From our results, all four antibodies reacted with monomeric BIGH3, WT, R124C, R124H, L518P, and L527R. In addition, these antibodies detected oligomeric or polymeric TGFBIp when present. We further confirmed that the purified TGFBIp, especially $(His)_6$-TGFBI-Strep (2-tag protein), is prone to aggregation and that TGFBIp oligomerization is primarily associated with purified proteins but less with cell lysates. We speculate that the presence of other non-TGFBIp proteins in cell lysates may act as a protein chaperone to prevent TGFBIp aggregation. Nevertheless, such a speculation regarding interference of TGFBIp aggregation awaits further investigation.

In this study, we have also identified several unique TGFBIp fragments potentially responsible for amyloid aggregates in LCD. Most interestingly, a 47-kDa band was detected in purified 2-tag L518P protein by all four anti-TGFBIp antibodies raised against different regions of TGFBIp (Figs. 1, 2). However, such a fragment was not detected in the purified proteins or cell lysates of 1-tag L518P. The fact that this fragment was detected by all four antibodies in 2-tag L518P proteins highly suggests the 47-kDa fragment is indeed a component of TGFBIp and most likely containing the a.a. 30 to approximately 518. It may be ubiquitously present in the protein aggregates of LCD related to L518P. Furthermore, a 43-kDa band was detected predominantly by KE50 and the anti-TGFBIp antibody (Proteintech Group) in purified 2-tag proteins of R124C and R124H (Figs. 1, 2) as well as in 1-tag purified proteins and cell lysates of R124C (Figs. 3, 4). These findings also suggest that the 43-kDa fragment is a component of TGFBIp in proximity to the N-terminus. Because it is present in at least R124C and R124H, this 43-kDa fragment may represent a marker for LCD variants.

As shown by these four antibodies, BIGH3, recombinant WT TGFBIp, and mutants can all oligomerize and lead to protein aggregations that are likely to be the primary proteinous component observed in corneal opacities associated with TGFBIp-related LCD. Moreover, our result is different from previous findings that wild-type and mutant TGFBI proteins all displayed similar degradation patterns by immunoprecipitation and Western blot analysis when expressed in transfected corneal epithelial cells and CHO cells.[35,36] We find that differential degradation does exist between recombinant WT and four mutant proteins (R124C, R124H, L518P, and L527R), as indicated by the above-cited findings of several previously unreported TGFBIp-related fragments. In addition to a 47-kDa fragment detected only in L518P by all four antibodies, we found a 43-kDa fragment in both $(His)_6$-TGFBIp purified protein and cell lysates of R124C and $(His)_6$-TGFBI-Strep proteins of R124H by all four antibodies. As discussed earlier, R124C is usually associated with LCD1 and only amyloid deposits, whereas R124H is associated with GCD2 and a more complex stromal aggregation of both granular (nonamyloid) and lattice (amyloid) deposits. We speculate that these degradation products of TGFBIp may be an important contributing factor to the amyloid deposits commonly observed in corneas with LCD1 and GCD2. At the same time, our findings support the notion that accumulation of degraded TGFBIp products is crucial in the pathogenesis of *TGFBI*-related corneal dystrophies. Takács et al.[20] previously suggested that altered processing of mutated TGFBIp results in 42-kDa protein constituting the amyloid deposition in LCD1. Our data also demonstrate that protein aggregates derived from recombinant TGFBIp contain not only the full-length proteins but also smaller fragments. Such a notion is also consistent with the in vivo findings of Stix et al.[22]

In principle, mutations in *TGFBI* could affect corneal opacity by interfering with protein folding and/or by altering binding interactions of TGFBIp. A mutation in the protein core may have either a subtle effect on protein stability slowly manifesting over time or a dramatic effect, where the protein is improperly folded and not secreted.[37] In the former case, the TGFBIp may become insoluble and aggregate, perhaps with other extracellular matrix proteins. In the latter case, there may be an adverse effect on binding partners due to the decreased amount of TGFBIp available for binding. Clout and Hohenester[37] have established a structural model of the fourth FAS1 domain of TGFBIp and concluded that, with the exception of R124 and R555, all mutation sites implicated so far in TGFBIp-related dystrophy are highly conserved and probably have a role in protein folding and maintenance of protein structure. The common mutations at positions R124 and R555 may directly affect protein–protein interactions (either homo- or heterophilic), whereas the rare mutations are likely to cause misfolding within the cell. In some of the latter cases, it is possible that mutant proteins escape the surveillance of the secretory pathways, but they will be severely destabilized and unable to withstand the harsh extracellular milieu.

An important question with regard to various *TGFBI* mutations that remains unanswered is why amyloids are formed with certain mutations, whereas other mutations, even those involving the same residue, as in the case of Arg124, are not as amyloidogenic. Studies with synthetic peptides of TGFBIp have shown that those peptides with cysteine at position 124 form a greater degree of amyloids than those with histidine, serine, or arginine.[38,39] The tendency for amyloid formation has been attributed to the hydrophobic character of the mutated protein (contributed by valine112 and valine113), the formation of cystine–disulfide bonds, and potential for H-bonding.[39] In vivo, it is possible that specific degradation products of mutant TGFBIp predispose to amyloid formation. Since different combinations of proteolytic fragments of TGFBIp have been observed in the corneas with Arg124Cys, Arg124Leu, or Arg124His mutations,[31] the mutations may alter the protein degradation in specific ways, and thereby have differential effects on the structure and stability of the deposited proteins. Interestingly, in patients with TGFBIp-related corneal dystrophies, mutant TGFBIp do not form amyloid deposits in the skin or other tissues, indicating that TGFBIp may be involved in corneal-specific protein–protein interactions.[40,41] It is also possible that tissue-specific factors are responsible for the turnover of mutant TGFBIp.[42] Other innate characteristics, aside from protein catabolism/degradation, are also likely contributors to cornea-specific abnormal aggregation of mutant TGFBIp, as previously suggested by other authors.[37,39,43] Nonetheless, point mutations in the gene encoding for this protein are probably not the only reason for amyloid formation under these circumstances. Future work is warranted to characterize the modulatory mechanisms responsible for the formation of amyloid or nonamyloid aggregates in TGFBIp-related corneal dystrophies.

Although the behavior of synthetic peptides or recombinant proteins in vitro is not necessarily similar to that of a full-length protein in vivo, our findings are in agreement with most of the phenotype–genotype associations observed in clinical reports. It is yet to be determined whether proteolytic fragments containing the amyloidogenic regions such as those identified by us are present and involved in the in vivo amyloid fibril formation. The abnormal protein aggregations in TGFBI-related corneal dystrophies may be mediated by these putatively amyloidogenic regions via alternative mechanisms such as mutation-induced protein unfolding and/or abnormal degradation. Further studies of biochemical properties of TGFBIp mutant proteins and identification of cornea-specific factors that favor deposition of such proteins will help us better understand the pathogenesis of TGFBIp-related corneal dystrophies.[44] If one could manage to recognize these factors, it would enable more effective therapeutic strategies to circumvent the formation of untoward

protein aggregates and ameliorate visual impairment of those affected individuals.

References

1. Skonier J, Neubauer M, Madisen L, et al. cDNA cloning and sequence analysis of beta ig-h3, a novel gene induced in a human adenocarcinoma cell line after treatment with transforming growth factor-beta. *DNA Cell Biol.* 1992;11:511–522.
2. Escribano J, Hernando N, Ghosh S, Crabb J, Coca-Prados M. cDNA from human ocular ciliary epithelium homologous to beta ig-h3 is preferentially expressed as an extracellular protein in the corneal epithelium. *J Cell Physiol.* 1994;160:511–521.
3. Rawe IM, Zhan Q, Burrows R, et al. Beta-ig. Molecular cloning and in situ hybridization in corneal tissues. *Invest Ophthalmol Vis Sci.* 1997;38:893–900.
4. LeBaron RG, Bezverkov KI, Zimber MP, et al. Beta IG-H3, a novel secretory protein inducible by transforming growth factor-beta, is present in normal skin and promotes the adhesion and spreading of dermal fibroblasts in vitro. *J Invest Dermatol.* 1995;104:844–849.
5. Kitahama S, Gibson MA, Hatzinikolas G, et al. Expression of fibrillins and other microfibril-associated proteins in human bone and osteoblast-like cells. *Bone.* 2000;27:61–67.
6. Ferguson JW, Thoma BS, Mikesh MF, et al. The extracellular matrix protein betaIG-H3 is expressed at myotendinous junctions and supports muscle cell adhesion. *Cell Tissue Res.* 2003;313:93–105.
7. Ohno S, Doi T, Fujimoto K, et al. RGD-CAP (betaig-h3) exerts a negative regulatory function on mineralization in the human periodontal ligament. *J Dent Res.* 2002;81:822–825.
8. Carson DD, Lagow E, Thathiah A, et al. Changes in gene expression during the early to mid-luteal (receptive phase) transition in human endometrium detected by high-density microarray screening. *Mol Hum Reprod.* 2002;8:871–879.
9. Lee SH, Bae JS, Park SH, et al. Expression of TGF-beta-induced matrix protein beta ig-h3 is upregulated in the diabetic rat kidney and human proximal tubular epithelial cells treated with high glucose. *Kidney Int.* 2003;64:1012–1021.
10. Hirano K, Klintworth GK, Zhan Q, et al. Beta ig-h3 is synthesized by corneal epithelium and perhaps endothelium in Fuchs' dystrophic corneas. *Curr Eye Res.* 1996;15:965–972.
11. Runager K, Enghild JJ, Klintworth GK. Focus on molecules: transforming growth factor beta induced protein (TGFBIp). *Exp Eye Res.* 2008;87:298–299.
12. Klintworth GK. The molecular genetics of the corneal dystrophies: current status. *Front Biosci.* 2003;8:d687–d713.
13. Streeten BW, Qi Y, Klintworth GK, et al. Immunolocalization of beta ig-h3 protein in 5q31-linked corneal dystrophies and normal corneas. *Arch Ophthalmol.* 1999;117:67–75.
14. Weiss JS, Møller HU, Lisch W, et al. The IC3D classification of the corneal dystrophies. *Cornea.* 2008;27:S1–S42.
15. Munier FL, Korvatska E, Djemai A, et al. Kerato-epithelin mutations in four 5q31-linked corneal dystrophies. *Nat Genet.* 1997;15:247–251.
16. Endo S, Nguyen TH, Fujiki K, et al. Leu518Pro mutation of the beta ig-h3 gene causes lattice corneal dystrophy type I. *Am J Ophthalmol.* 1999;128:104–106.
17. Kawasaki S, Nishida K, Quantock AJ, et al. Amyloid and Pro501 Thr-mutated (beta) ig-h3 gene product colocalize in lattice corneal dystrophy type IIIA. *Am J Ophthalmol.* 1999;127:456–458.
18. Fujiki K, Hotta Y, Nakayasu K, et al. A new L527R mutation of the betaIGH3 gene in patients with lattice corneal dystrophy with deep stromal opacities. *Hum Genet.* 1998;103:286–289.
19. Dighiero P, Drunat S, Ellies P, et al. A new mutation (A546T) of the betaig-h3 gene responsible for a French lattice corneal dystrophy type IIIA. *Am J Ophthalmol.* 2000;129:248–251.
20. Takács L, Boross P, Tözser J, et al. Transforming growth factor-beta induced protein, betaIG-H3, is present in degraded form and altered localization in lattice corneal dystrophy type I. *Exp Eye Res.* 1998;66:739–745.
21. Zerovnik E. Amyloid-fibril formation. Proposed mechanisms and relevance to conformational disease. *Eur J Biochem.* 2002;269:3362–3371.
22. Stix B, Leber M, Bingemer P, et al. Hereditary lattice corneal dystrophy is associated with corneal amyloid deposits enclosing C-terminal fragments of keratoepithelin. *Invest Ophthalmol Vis Sci.* 2005;46:1133–1139.
23. Rochet JC. Novel therapeutic strategies for the treatment of protein-misfolding diseases. *Expert Rev Mol Med.* 2007;9:1–34.
24. Takács L, Losonczy G, Matesz K, et al. TGFBI (BIGH3) gene mutations in Hungary: report of the novel F547S mutation associated with polymorphic corneal amyloidosis. *Mol Vis.* 2007;13:1976–1983.
25. Korvatska E, Munier FL, Chaubert P, et al. On the role of keratoepithelin in the pathogenesis of 5q31-linked corneal dystrophies. *Invest Ophthalmol Vis Sci.* 1999;40:2213–2219.
26. Kim JE, Han MS, Bae YC, et al. Anterior segment dysgenesis after overexpression of transforming growth factor-beta-induced gene, beta igh3, in the mouse eye. *Mol Vis.* 2007;13:1942–1952.
27. Grothe HL, Little MR, Cho AS, et al. Denaturation and solvent effect on the conformation and fibril formation of TGFBIp. *Mol Vis.* 2009;15:2617–2626.
28. Yuan C, Reuland JM, Lee L, et al. Optimized expression and refolding of human keratoepithelin BL21 (DE3). *Protein Expr Purif.* 2004;35:39–45.
29. Patel DA, Chang SH, Harocopos GJ, et al. Granular and lattice deposits in corneal dystrophy caused by R124C mutation of TGFBIp. *Cornea.* 2010;29:1215–1222.
30. Atchaneeyasakul LO, Appukuttan B, Pingsuthiwong S, et al. A novel H572R mutation in the transforming growth factor-beta-induced gene in a Thai family with lattice corneal dystrophy type I. *Jpn J Ophthalmol.* 2006;50:403–408.
31. Korvatska E, Henry H, Mashima Y, et al. Amyloid and non-amyloid forms of 5q31-linked corneal dystrophy resulting from keratoepithelin mutations at Arg-124 are associated with abnormal turnover of the protein. *J Biol Chem.* 2000;275:11465–11469.
32. Dobson CM. Protein misfolding, evolution and disease. *Trends Biochem Sci.* 1999;24:329–332.
33. Fändrich M, Fletcher MA, Dobson CM. Amyloid fibrils from muscle myoglobin. *Nature.* 2001;410:165–166.
34. Munishkina LA, Fink AL, Uversky VN. Conformational prerequisites for formation of amyloid fibrils from histones. *J Mol Biol.* 2004;342:1305–1324.
35. Kim JE, Park RW, Choi JY, et al. Molecular properties of wild type and mutant betaIG-H3 proteins. *Invest Ophthalmol Vis Sci.* 2002;43:656–661.
36. Morand S, Buchillier V, Maurer F, et al. Induction of apoptosis in human corneal and HeLa cells by mutated BIGH3. *Invest Ophthalmol Vis Sci.* 2003;44:2973–2979.
37. Clout NJ, Hohenester E. A model of FAS1 domain 4 of the corneal protein beta (ig)-h3 gives a clearer view on corneal dystrophies. *Mol Vis.* 2003;9:440–448.
38. Schmitt-Bernard CF, Chavanieu A, Derancourt J, et al. In vitro creation of amyloid fibrils from native and Arg124Cys mutated beta IGH3 (110–131) peptides, and its relevance for lattice corneal amyloid dystrophy type I. *Biochem Biophys Res Commun.* 2000;273:649–653.
39. Schmitt-Bernard CF, Chavanieu A, Herrada G, et al. BIGH3 (TGFBI) Arg124 mutations influence the amyloid conversion of related peptides in vitro. *Eur J Biochem.* 2002;269:5149–5156.
40. Schmitt-Bernard CF, Schneider C, Argilés A. Clinical, histopathologic, and ultrastructural characteristics of BIGH3 (TGFBI) amyloid corneal dystrophies are supportive of the existence of a new type of LCD: the LCDi. *Cornea.* 2002;21:463–468.
41. El Kochairi I, Letovanec I, Uffer S, Munier FL, Chaubert P, Schorderet DF. Systemic investigation of keratoepithelin deposits in TGFBI/BIGH3-related corneal dystrophy. *Mol Vis.* 2006;12:461–466.
42. Kannabiran C, Klintworth GK. TGFBI gene mutations in corneal dystrophies. *Hum Mutat.* 2006;27:615–625.
43. Suesskind D, Auw-Haedrich C, Schorderet DF, et al. Keratoepithelin in secondary corneal amyloidosis. *Graefes Arch Clin Exp Ophthalmol.* 2006;244:725–731.
44. Yuan C, Berscheit HL, Huang AJ. Identification of an amyloidogenic region on keratoepithelin via synthetic peptides. *FEBS Lett.* 2007;581:241–247.